Design of large π-conjugated α-cyanostilbenes derivatives as colorimetric sensors for volatile acids and organic amines gases

Xinhua Cao,* Yiran Li, Qingqing Han, Aiping Gao, Bingya Wang, Xueping Chang and Ji-ting Hou*

College of Chemistry and Chemical Engineering, Henan Province Key Laboratory of Utilization of Non-metallic Mineral in the South of Henan & Green catalysis and synthesis key laboratory of Xinyang city, Xinyang Normal University, 237 Southlake Road, Xinyang 464000, P. R. China

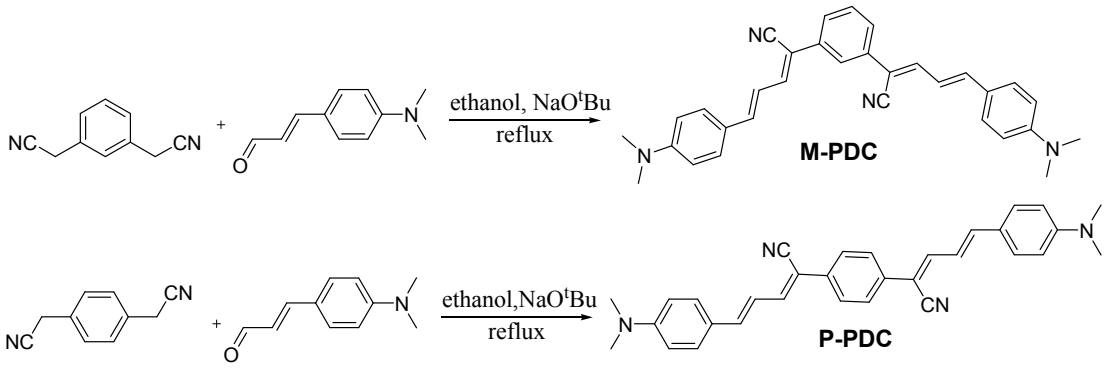

Scheme S1 The synthesis routine of **M-PDC** and **P-PDC**.

Synthesis of M-PDC: m-Phenylenediacetonitrile (1.00 g, 6.40 mmol), 4-dimethylaminocinnamaldehyde (2.24 g, 12.80 mmol) and sodium-t-butoxide (1.84 g, 19.20 mmol) were added to anhydrous ethanol (25 mL). The mixture was heated to reflux and kept overnight. After the reaction was over, a large precipitate was produced. The precipitate was filtrated and washed with ethanol for many times. The reddish brown powder was obtained with the yield of 70%. ^{1}HNMR (600 MHz, $CDCl_3$): 7.75 (s, 1H), 7.53 (d, J = 8.4 Hz, 2H), 7.47 (d, J = 8.4 Hz, 6H), 7.41 (t, J = 7.8 Hz, 4H), 7.20 (t, J = 11.4 Hz, 2H), 7.02 (s, 1H), 6.99 (s, 1H), 6.69 (d, J = 9.0 Hz, 4H), 3.03 (s, 12H), ^{13}CNMR (150 MHz, $CDCl_3$): 151.5, 145.7, 143.9, 143.7, 143.1, 140.2, 134.7, 131.2, 129.5, 125.2, 123.7, 120.6,118.1, 40.3. HRMS calculated for $C_{32}H_{31}N_4$ $[M+H]^+$ 471.2549, found: 471.2548.

Synthesis of P-PDC: p-Phenylenediacetonitrile (1.00 g, 6.40 mmol), 4-dimethylaminocinnamaldehyde (2.24 g, 12.80 mmol) and sodium-t-butoxide (1.84 g, 19.20 mmol) were added to anhydrous ethanol (25 mL). The mixture was heated to reflux and kept overnight. After the reaction was over, a large precipitate was produced. The precipitate was filtrated and washed with ethanol for many times. The nut-brown powder was obtained with the yield of 77%. ^{1}HNMR (600 MHz, $CDCl_3$): 7.66 (d, J = 8.4 Hz, 1H), 7.60 (d, J = 4.8 Hz, 2H), 7.53 (d, J = 8.4 Hz, 1H), 7.47-7.42 (m, 4H), 7.33 (d, J = 8.4 Hz, 1H), 7.22-7.12 (m, 2H), 7.01 (t, J = 8.4 Hz, 2H), 6.92 (d, J = 15.0 Hz, 1H), 6.74 (d, J = 8.4 Hz, 1H), 6.69 (d, J = 8.4 Hz, 3H), 6.65 (d, J = 8.4 Hz, 1H), 3.03 (s, 12H), ^{13}CNMR (150 MHz, $CDCl_3$): 151.5, 143.1, 142.8, 133.7, 129.6, 129.4, 125.7, 125.5, 123.8, 120.7, 117.8, 40.3. HRMS calculated for $C_{32}H_{31}N_4$ $[M+H]^+$ 471.2549, found: 471.2548.

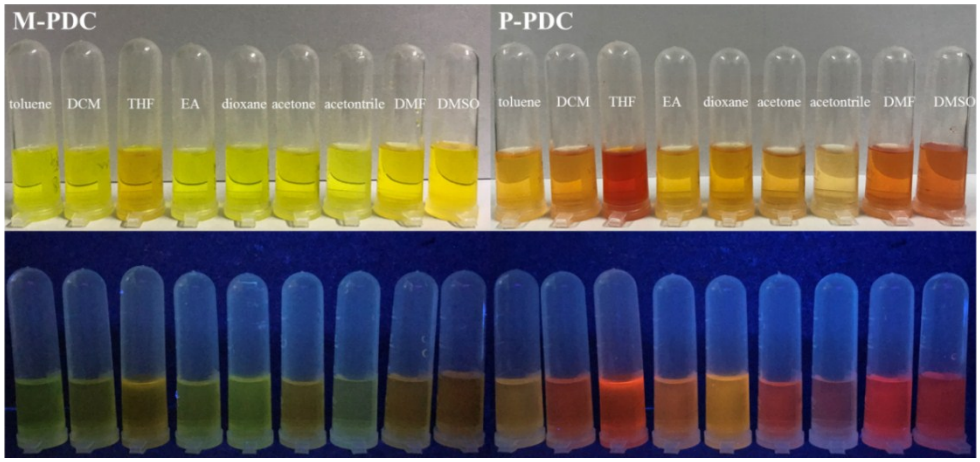

Fig. S1 The visual images of solutions **M-PDC** and **P-PDC** in different solvents. The upper and lower were under daylight and 365 nm light, respectively. The solution concentration was all 10^{-5} M.

Table S1 The photophysical properties of **M-PDC** and **P-PDC** in different solvents.

compound / solvent	Absorption band (nm)		Log ε (L mol^{-1} cm^{-1})		Fluorescence intensity (nm)	
	M-PDC	**P-PDC**	**M-PDC**	**P-PDC**	**M-PDC**	**P-PDC**
dioxane	428	469	4.84	4.81	546	580
toluene	435	476	4.87	4.51	543	601
acetontrile	436	472	4.80	4.18	582	656
ethyl acetate	426	469	5.01	4.46	557	610
DMF	443	488	4.88	4.77	586	665
THF	432	476	4.82	4.81	562	617
acetone	434	475	4.70	4.36	577	645
CH_2Cl_2	437	474	4.46	4.73	562	617
DMSO	452	489	5.05	4.84	594	674

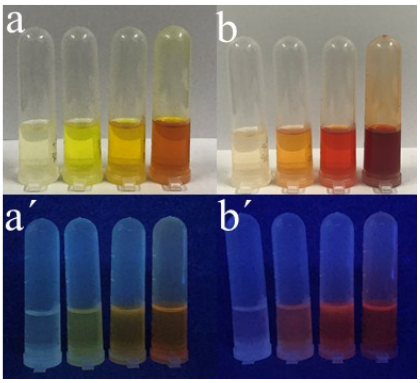

Fig. S2 The visual images of solutions **M-PDC** (a and a´) and **P-PDC** (b and b´) in CH_2Cl_2 with different concentration. The upper and lower were under daylight and 365 nm light, respectively. The concentration of solution **M-PDC** and **P-PDC** from left to right were 10^{-6}, 10^{-5}, 10^{-4} and 10^{-3} M.

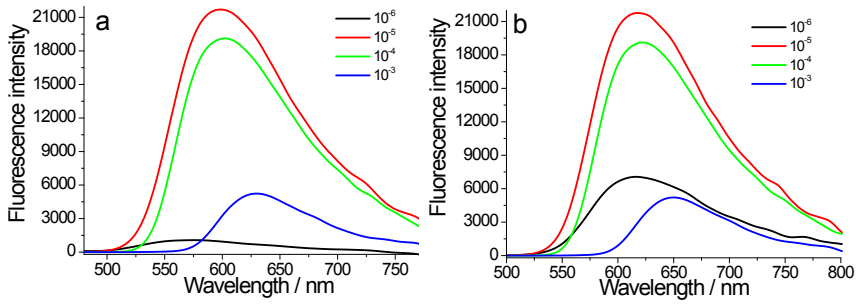

Fig. S3 Concentration-dependent fluorescence emission spectra of solutions **M-PDC** (a) and **P-PDC** (b) in CH_2Cl_2.

Table S2 The quantum yields and fluorescence lifetime of **M-PDC** and **P-PDC** in different solvents.

compound / solvent	QY%		Lifetime (ps)	
	M-PDC	**P-PDC**	**M-PDC**	**P-PDC**
dioxane	0.51	2.39	70	201.0
toluene	4.73	4.78	54	211.1
acetonitrile	1.14	1.87	75	276.9
ethyl acetate	--	1.39	29	226.7
DMF	1.53	5.03	53	378.6
THF	--	1.24	48	223.9
acetone	1.83	2.02	58	268.9
CH_2Cl_2	--	1.14	39	199.7
DMSO	0.18	3.96	33	316.6

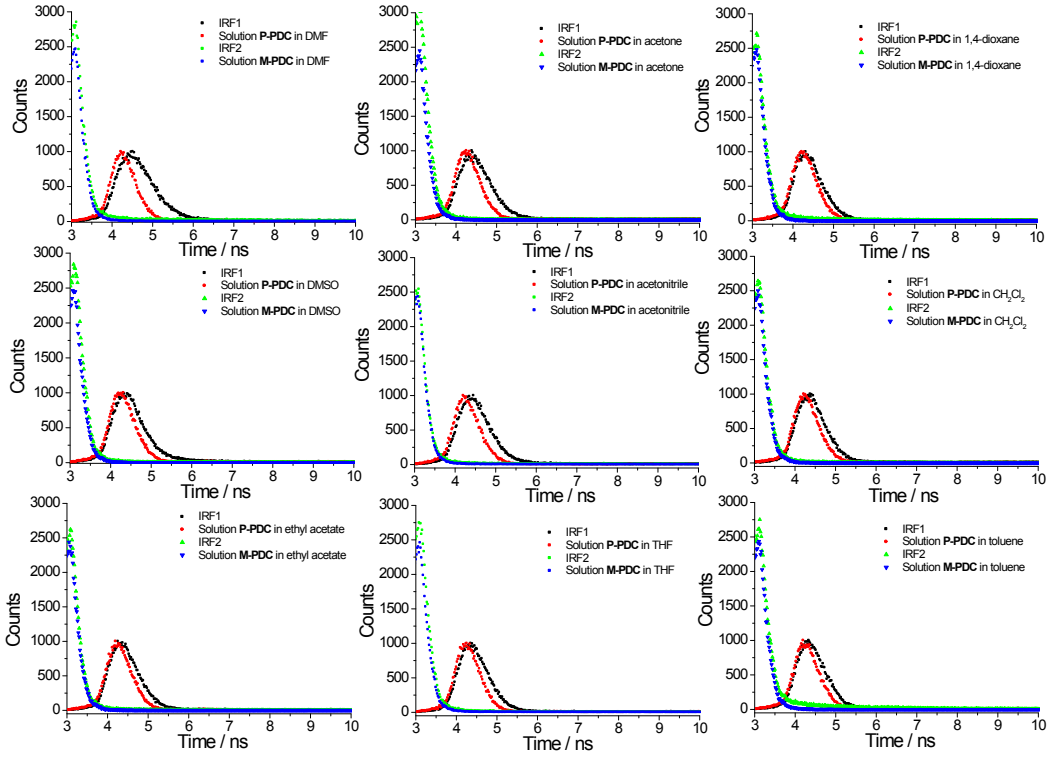

Fig. S4 Lifetime decay profiles (λex = 450 nm,monitored at their maximum emission wavelength) of **M-PDC** and **P-PDC** in different solvents. The solution concentration was all 10^{-5} M.

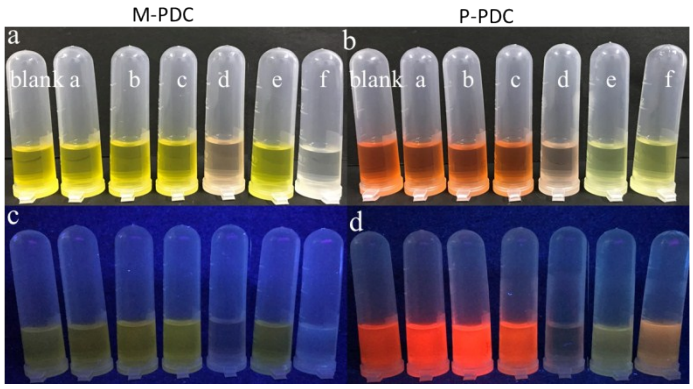

Fig. S5 The visual images of solutions **M-PDC** and **P-PDC** in CH_2Cl_2 with addition of different volatile acids: a) formic acid; b) acetic acid; c) propionic acid; d) HNO_3; e) HCl; f) TFA. The solution concentration was all 10^{-5} M.

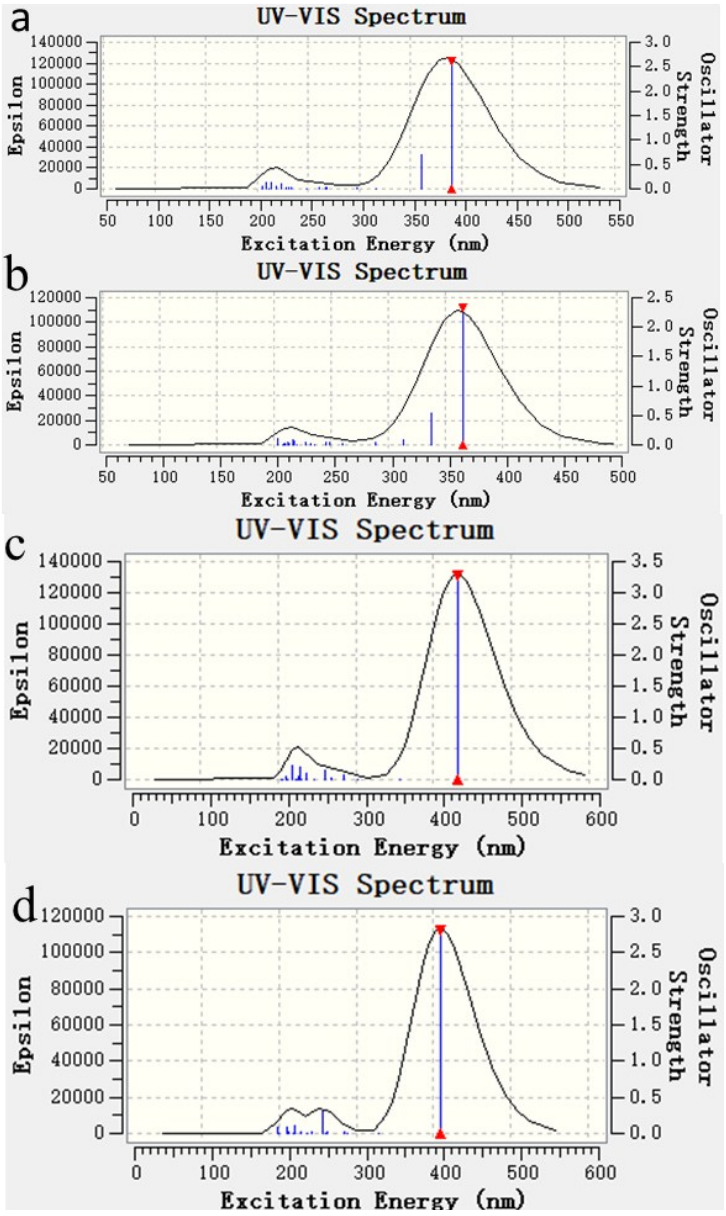

Fig. S6 The absorption spectra of **M-PDC** and **P-PDC** and complexes **M-PDC-2H** and **M-PDC-2H** obtained from DFT calculation: a) for compound **M-PDC**, b) for complex **M-PDC-2H**, c) for compound **P-PDC**, d) for complex **P-PDC-2H**.

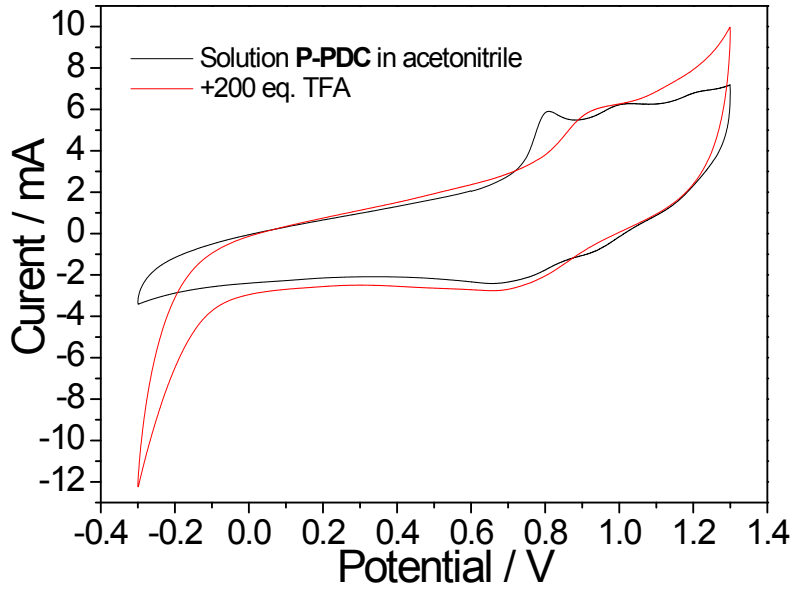

Fig. S7. Cyclic voltammograms of solution **P-PDC** (10^{-5} M) in acetonitrile with gradual addition of TFA in the present of 0.5 M tetrabutylammonium hexafluorophosphate as electrolyte.

Table S3 Detection limit of **M-PDC** toward TFA and TEA in CH_2Cl_2 by absorbance changes at 437 nm

n	1	2	3	4	5	6	7	8	9	10	11
Absorbance (Xn)	1.739	1.740	1.739	1.739	1.738	1.739	1.740	1.738	1.738	1.740	1.741

$X_{average} = 1.739$ $\sigma_{wb} = sqrt(\sum(X_n-X_{average})^2/n) = 8.8\times10^{-7}$

The detection limit: [TFA] = 3σ/b = 2.0 nM

[TEA] = 3σ/b = 1.76 nM

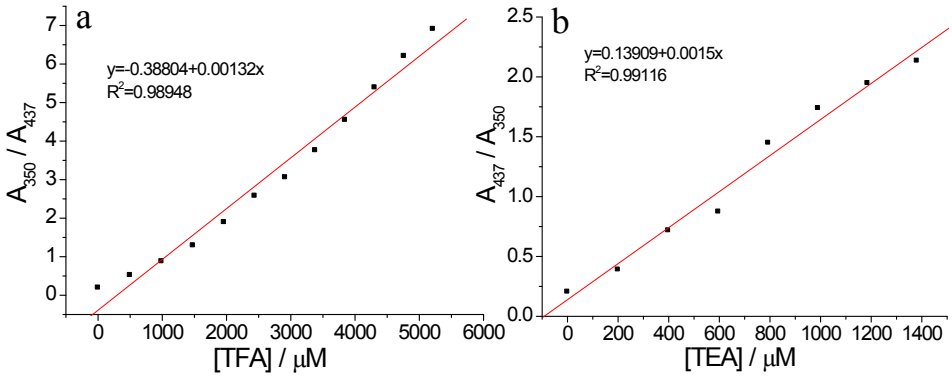

Fig. S8 The linear fitting curve of absorbance change of **M-PDC** solution with the addition of TFA (a) and **M-PDC** with 550.0 eq. of TFA with addition of TEA (b).

Table S4 Detection limit of **P-PDC** toward TFA and TEA in CH_2Cl_2 by absorbance changes at 485 nm

n	1	2	3	4	5	6	7	8	9	10	11
Absorbance (Xn)	0.787	0.787	0.786	0.786	0.786	0.785	0.785	0.788	0.789	0.789	0.784

$X_{average}$ = 0.786545 $\sigma_{wb} = sqrt(\sum(X_n-X_{average})^2/n)$ = 0.00000243

The detection limit: [TFA] = 3σ/b = 8.82 nM

[TEA] = 3σ/b = 3.47 nM

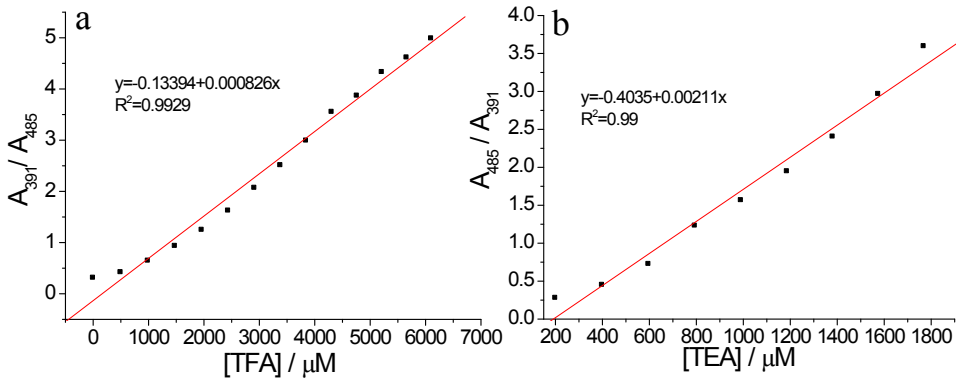

Fig. S9 The linear fitting curve of absorbance change of solution **P-PDC** with the addition of TFA (a) and **P-PDC** with 650.0 eq. of TFA with addition of TEA.

Table S5 Detection limit of film **M-PDC**+CTAB toward TFA gas by fluorescence emission changes at 611 nm.

n	1	2	3	4	5	6	7	8	9	10	11
Intensity (Xn)	326.0	325.9	325.7	325.1	325.1	326.3	325.7	325.3	325.1	325.1	326.0

$X_{average}$ = 325.6 $\sigma_{wb} = sqrt(\sum(X_n-X_{average})^2/n)$ = 0.181983

The detection limit: [TFA] = 3σ/b = 17.4 ppm

Table S6 Detection limit of film **P-PDC**+CTAB toward TFA gas by fluorescence emission changes at 672 nm

n	1	2	3	4	5	6	7	8	9	10	11
Intensity (Xn)	207.9	208.0	208.0	207.8	208.0	207.8	208.3	207.8	207.7	208.3	207.6

$X_{average}$ = 207.9 $\sigma_{wb} = sqrt(\sum(X_n-X_{average})^2/n)$ = 0.04561983

The detection limit: [TFA] = 3σ/b = 2.37 ppm

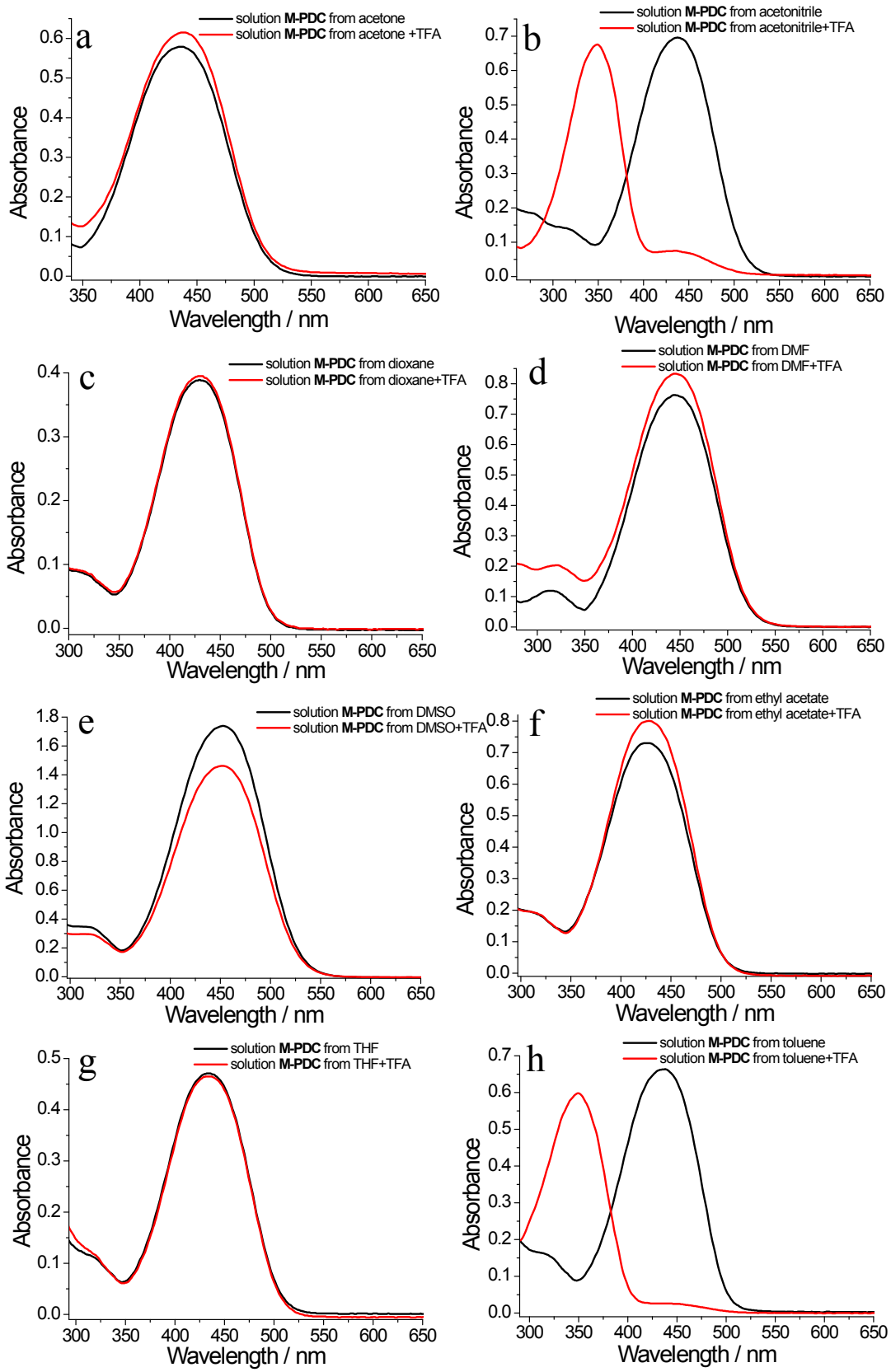

Fig. S10 UV-vis absorption spectra of solution **M-PDC** in different solvents before and after addition of 500 eq. of TFA. The concentration of solution **M-PDC** in different solvents was 10^{-5} M.

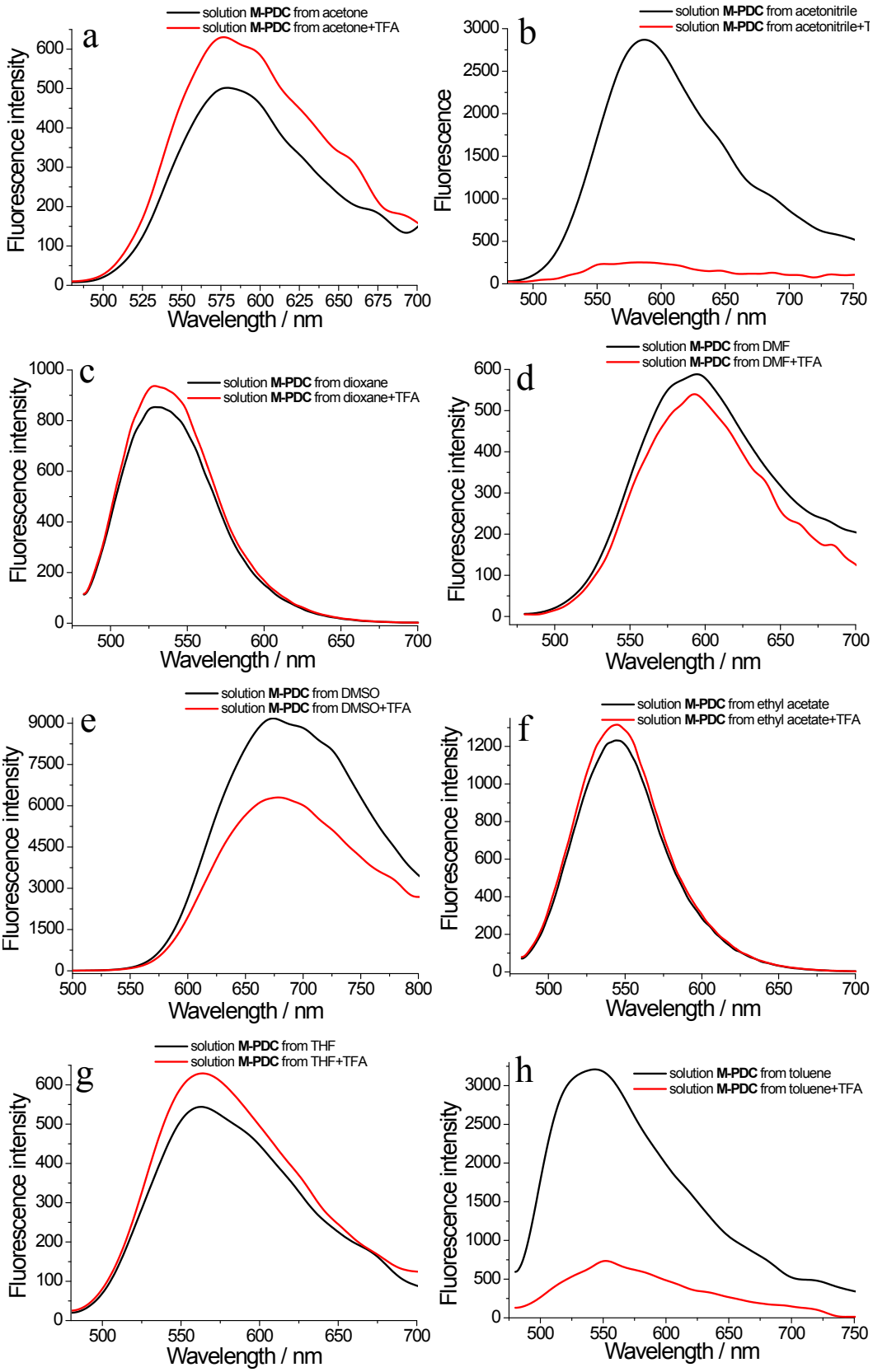

Fig. S11 Fluorescence emission spectra of solution M-PDC in different solvent before and after addition of 500 eq. of TFA. The concentration of solution **M-PDC** in different solvents was 10^{-5} M.

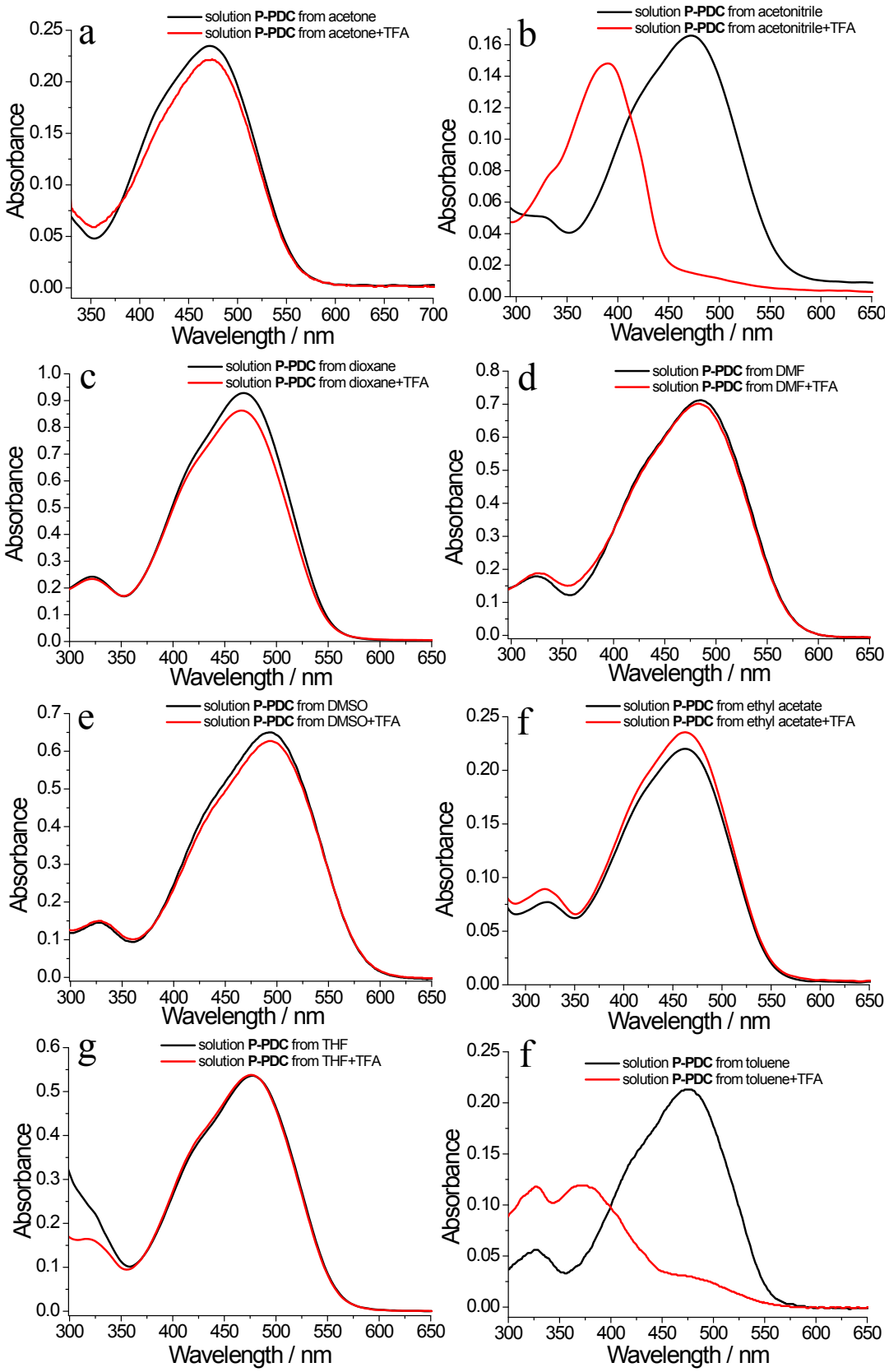

Fig. S12 UV-vis absorption spectra of solution **P-PDC** in different solvent before and after addition of 500 eq. of TFA. The concentration of solution **P-PDC** in different solvents was 10^{-5} M.

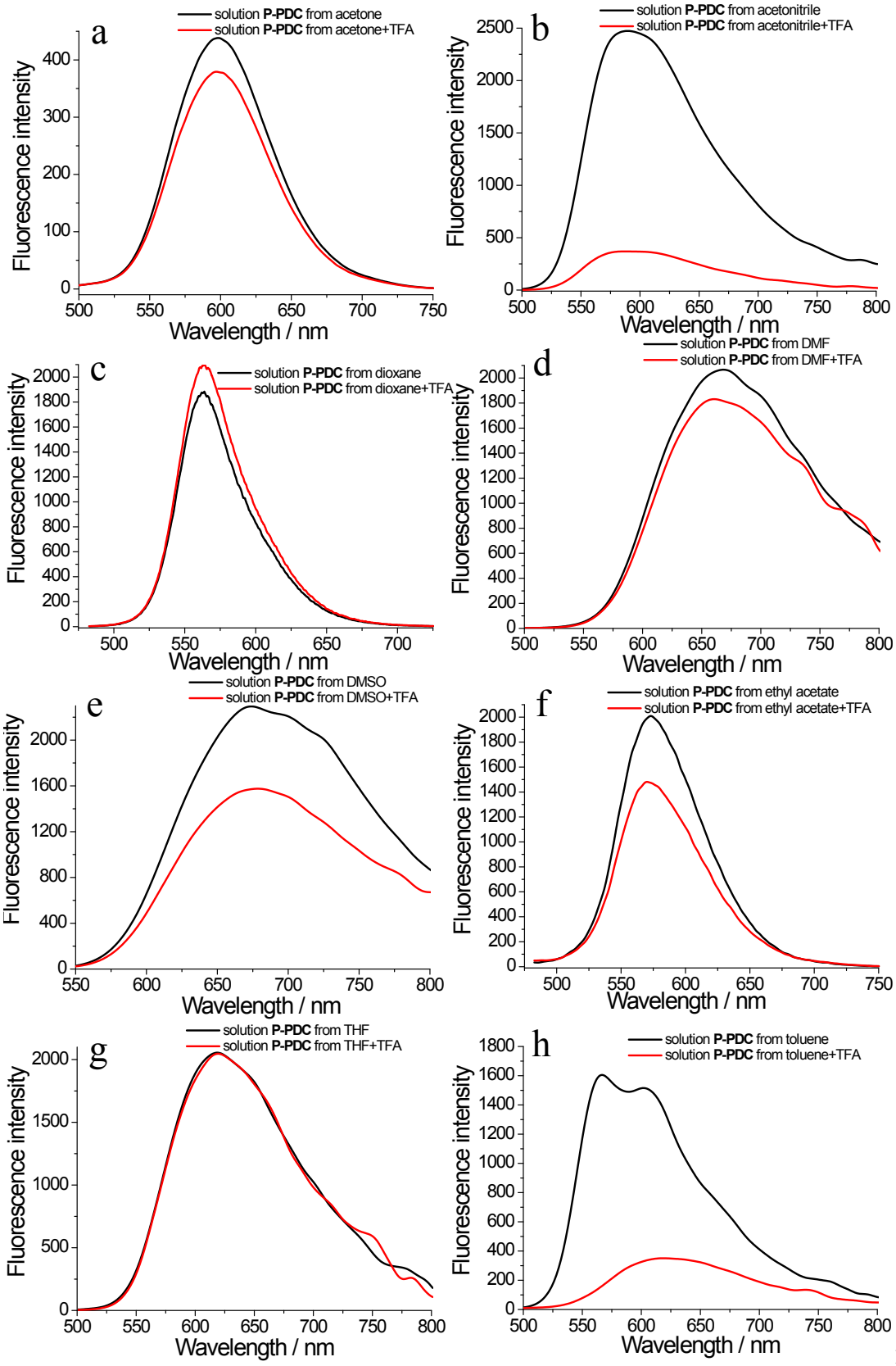

ig. S13 Fluorescence emission spectra of solution **P-PDC** in different solvent before and after addition of 500 eq. of TFA. The concentration of solution **P-PDC** in different solvents was 10^{-5} M.

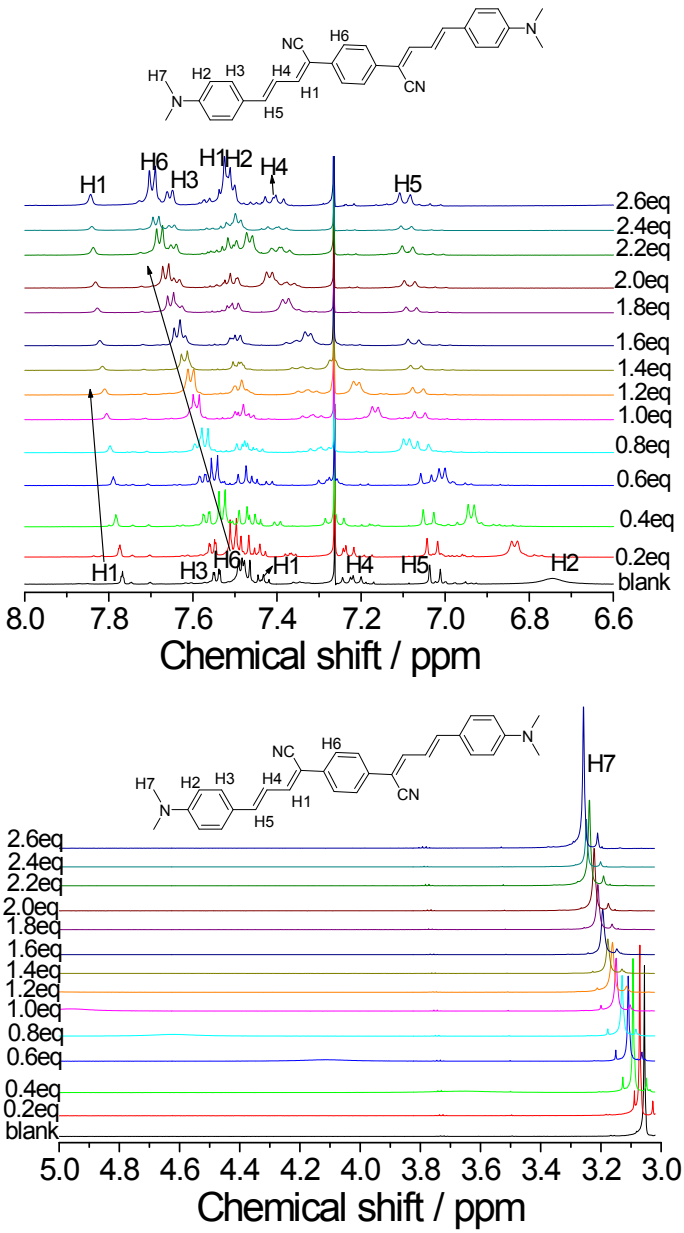

Fig. S14 ^{1}HNMR titration of **P-PDC** in $CDCl_3$ by CF_3COOH (0-2.6 eq.).

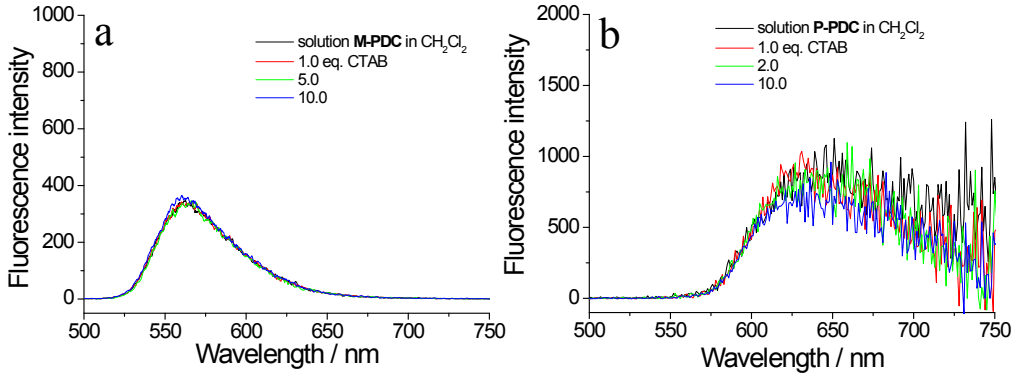

Fig. S15 Fluorescence emission spectra change of solutions **M-PDC** (a) and **P-PDC** (b) in CH_2Cl_2 (10^{-3} M)

with addition of different amount of CTAB.

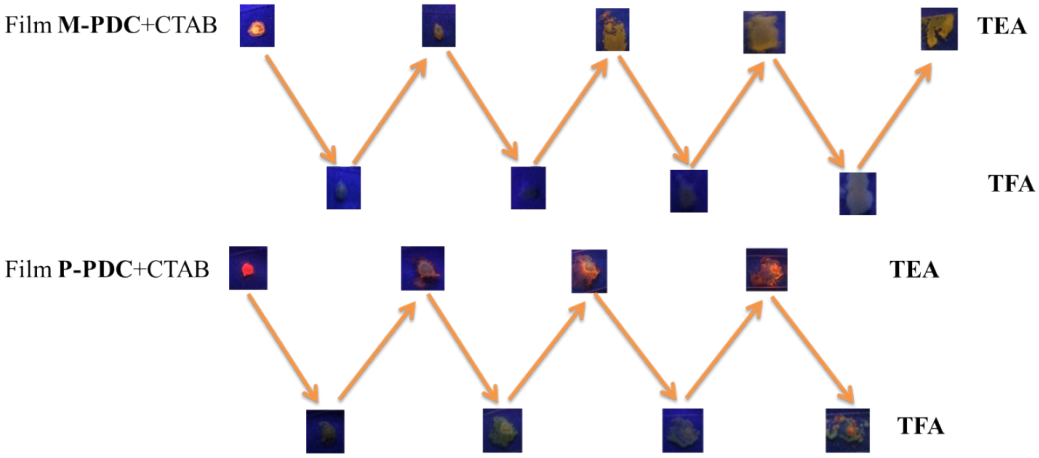

Fig. S16 Images of films **M-PDC**+CTAB and **P-PDC**+CTAB with contacting TFA and TEA gases in turn.

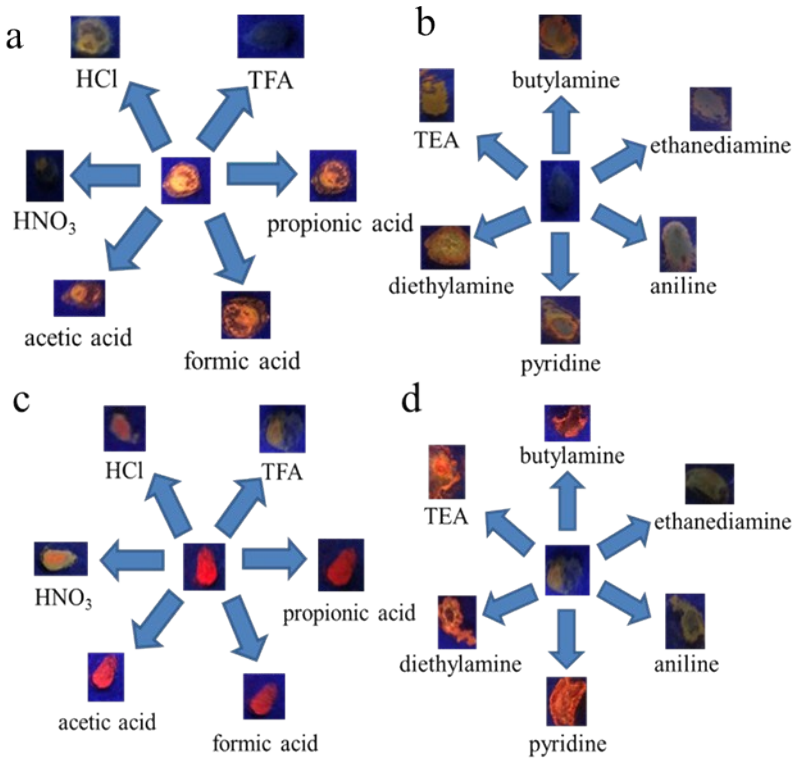

Fig. S17 Images of film **M-PDC**+CTAB (a and b) and **P-PDC**+CTAB (c and d) from CH_2Cl_2 with different gaseous acids and then organic amine vapors.

Fig. S18 The schematic of the test device.